Ionization of uranium atoms by electron impact

Jeffrey C. Halle,* H. H. Lo,† and Wade L. Fite
Department of Physics and Astronomy, University of Pittsburgh, Pittsburgh, Pennsylvania 15260
(Received 1 September 1978; revised manuscript received 24 October 1980)

The cross sections for single and multiple ionization of uranium by electron impact for energies 7.5–500 eV have been measured using a modulated crossed-beam experiment. The absolute total ionization cross section was found by comparing the cross section for ionization to the cross section for associative ionization in the reaction $U + O_2 \rightarrow UO_2^+ + e$. The total ion number cross section has a maximum value of $(5.8 \pm 0.9) \times 10^{-16}$ cm^2 occurring at an energy of about 50 eV. The single ionization cross section has a maximum of $(4.80 \pm 1.24) \times 10^{-16}$ cm^2 at an energy of 27 ± 5 eV. The cross sections for higher-order ionization have values at 500 eV that are 49%, 33%, and 17% that of single ionization for $n = 2$, 3, and 4, respectively. These ratios are significantly higher than those for other elements for which data are available.

I. INTRODUCTION

Several studies have been made in recent years of such basic properties of uranium as energy levels,[1,2] ionization potentials,[3-5] cross sections for charge transfer,[6,7] and associative ionization of uranium with oxygen[8-10] and other gases.[11] Blackburn and Danielson[12] using electron impact measured the relative ionization cross sections and fragmentation of urnaium and uranium oxides for electron energies greater than 60 eV. Theoretical sutdies in particular are very difficult due to extreme complexity of the uranium atom. In the ground state U($^5L_6^0$) there is one $6d$ electron with a binding energy 6.11 eV, two $7s$ electrons with binding energy 6.15 eV, and three $5f$ electrons with binding energy 8.18 eV.[1,13] There are 1900 known energy levels of U*I* and 270 known levels of U*II*, many of which are only a fraction of an electron volt above the ground state.[1,2] This complexity is heightened in any experiment. To vaporize uranium requires a temperature of 2000 K or more and this is sufficiently high to thermally populate the first excited state of U*I*, U($^5K_5^0$), which lies only 0.077 eV above the ground state. Similarly, U*II* has two levels, U($^6L_5^0$) and U($^6K_4^0$), which are only 0.036 and 0.11 eV, respectively, above the ground state configuration. Any accurate calculation to compare with experiment must include all of these configurations.

This paper describes the measurements of cross sections for the single and multiple ionizations of uranium atoms by electron impact in the reaction

$$U + e \rightarrow U^{n+} + (n+1)e \qquad (1)$$

for the electron energy range of 7.5-500 eV. These cross sections were normalized by comparing the results with the cross section for associative ionization of uranium with oxygen in the reaction

$$U + O_2 \rightarrow UO_2^+ + e. \qquad (2)$$

A comparison of these results to calculations based on typical theoretical formulas[13-15] demonstrates a marked difference between the shapes of the experimental and theoretical cross-section curves.

Two separate experiments were performed in this study. In the first the ratios of cross sections σ_{n+}^U, for producing U^{n+} ions where $n = 2$ to 4 to the cross section σ_+^U, for producing U^+, were measured at a series of electron energies and the shape of the cross-section curve as a function of electron energy was measured for σ_+^U. In the second experiment, the total cross section for electron-impact ionization was determined relative to the cross section for associative ionization with oxygen at selected energies.

II. EXPERIMENTAL APPROACH

A. Cross-section ratio and shape measurements

In this experiment, the ions were produced by electrons bombarding the uranium atoms in a crossed-beam ionizer. The ions were drawn into a quadrupole mass filter (QMF) which allowed transmission of only the specific ion desired. The transmitted ions were then detected as an ion current by an electron multiplier with a gain of about 10^5. In this manner, the relative amounts formed of each ion and the shapes of the cross-section curves could be measured as functions of electron energy.

In order to exclude residual gas ionizations signals, the uranium atom beam was interrupted at a fixed frequency of 19 Hz. Standard modulated beam techniques were then used to measure the modulated signal from the electron multiplier.

The ion signals measured are related to the cross section by

$$S_i^{U^{n+}}(E) = \sigma_{n+}^{U}(E) n_U l_i^U I_e(E) T(U,n), \quad (3)$$

where $S^{U^{n+}}$ is the signal produced by the U^{n+} ions, $\sigma_{n+}^{U}(E)$ is the cross section for production of U^{n+} at electron energy E, $I_e(E)$ is the electron current, l_i^U is the effective ionization path length of electrons in the uranium beam (see the Appendix), n_U is the uranium beam number density, and $T(U,n)$ is a measure of the combined transmission efficiency of the quadrupole and the gain of the multiplier. Thus the ratio of $\sigma_{n+}^{U}(E)$ to $\sigma_{+}^{U}(E)$ can be written

$$\frac{\sigma_{n+}^{U}}{\sigma_{+}^{U}}(E) = \frac{S_i^{U^{n+}}}{S_i^{U^{+}}}(E) \frac{T(U,1)}{T(U,n)}. \quad (4)$$

The gain of the multiplier is different for different values of n, and the transmission efficiency for the QMF is dependent on the charge-to-mass ratio of the ion. In order to account for these effects, a small mercury vapor source was introduced into the vacuum system. A few drops of mercury were placed in a well in a small aluminum block (~2 cm²) situated near the ionizer. The block was placed on a small resistive heater, which heated it slightly until mercury ion signal of desired intensity was observed. The increase in background pressure was not detectable by the ion gauge. The ratios of the various mercury ions were determined simultaneously with and in the same manner as for the uranium ions. Mercury was used because its ionization cross sections are well known, it is similar in mass to uranium, a necessary condition for proper calibration of the QMF, and it was already present in small amounts due to the mercury diffusion pumps used. By comparing the results using mercury to published data,[16] the transmission function ratio in Eq. (4) can be evaluated. This ratio is dependent on focusing and resolution settings, and was not necessarily reproducible from one day to the next. However, a criterion for acceptability of data was that this ratio be constant to within experimental uncertainties during the course of a run for different ionization energies and electron currents. For the lower energies at which the mercury ion signals were not observed, it was assumed that the transmission function remained constant. The mercury cross-section ratios, $\sigma_{n+}^{Hg}/\sigma_{+}^{Hg}$, used are listed in Table I.

To determine the shape of all the cross-section curves, it is sufficient to find the shape for only $n=1$. This was done by measuring the U^+ and Hg^+ signals at energy E and comparing them to the signals found at a set standard energy E_0. Thus the shape of $\sigma_+^U(E)$ is found from the formula

TABLE I. Mercury data [a] used to calibrate mass spectrometer.

E(eV)	$\sigma_{2+}^{Hg}/\sigma_{+}^{Hg}$ (10^{-2})	$\sigma_{3+}^{Hg}/\sigma_{+}^{Hg}$ (10^{-3})	$\sigma_{4+}^{Hg}/\sigma_{+}^{Hg}$ (10^{-3})	$\sigma_{+}^{Hg}(E)/\sigma_{+}^{Hg}(E_0)$
12.5				0.32
17.5				0.73
22.5				0.86
27.5	0.403			0.92
32.5	1.10			0.98
37.5	1.19			1.02
42.5	2.57			1.06
47.5	4.79			1.06
52.5	5.98			1.06
57.5	7.22			1.06
62.5	8.14			1.06
67.5	9.10			1.06
72.5	9.73			1.08
77.5	10.3			1.06
82.5	11.0	0.516		1.05
87.5	11.6	1.53		1.03
92.5	12.1	2.86		1.00
100	12.6	4.86		1.00
110	13.2	8.77		0.97
120	13.8	12.7		0.94
130	14.4	16.6		0.90
140	15.0	20.5		0.87
150	15.6	24.4		0.84
175	15.8	29.5		0.79
200	16.0	34.6	2.94	0.76
250	16.5	39.2	5.99	0.68
300	16.8	43.3	7.91	0.60
400	16.8	44.8	9.40	0.49
500	16.8	44.8	10.4	0.38

[a] From Ref. 16.

$$\frac{\sigma_+^U(E)}{\sigma_+^U(E_0)} = \frac{\sigma_+^{Hg}(E)}{\sigma_+^{Hg}(E_0)} \frac{S_i^{U^+}}{S_i^{Hg^+}}(E) \frac{S_i^{Hg^+}}{S_i^{U^+}}(E_0). \quad (5)$$

There were two reasons for determining the above cross-section ratio by using the Hg^+ signals rather than by the standard method in which the cross section is proportional to the signal per unit electron current. First, the method used here for $n=1$ is consistent with the method used for $n=2$ to 4. Second, the given method was more convenient than the standard method since electron current measurements were not required. As a check, the cross-section ratio frequently was determined using both methods; the correspondence was found to be within experimental error.

B. Absolute cross-section measurements

In the second experiment the total ionization cross section was measured at a few selected energies in order to determine the absolute values for the cross section σ_{n+}. The total cross section can be defined in one of two ways. The first is

charge weighted and is the electron production cross section,

$$\sigma_e = \sigma_+ + 2\sigma_{2+} + 3\sigma_{3+} + 4\sigma_{4+} + \cdots = \sum_n n\,\sigma_{n+}. \quad (6)$$

This is the total experimental cross section found by measuring the total ion current produced. The second is an ion-number cross section,

$$\sigma_{\text{ion}} = \sigma_+ + \sigma_{2+} + \sigma_{3+} + \sigma_{4+} + \cdots = \sum_n \sigma_{n+}. \quad (7)$$

This is the total cross section for producing ions and is proportional to the number of ions produced, not the current. Either designation is useful depending on context. In the second experiment the cross section in Eq. (6) was measured.

The uranium atoms passed between a set of horizontal parallel plates where they were bombarded by an electron beam. The ions produced were swept by an electric field to the top plates, where the total ion current was measured. The uranium beam was modulated in order to differentiate between the uranium ion signal and the signal produced by electron-impact ionization of the background gas, there being no mass analysis of the ions.

Alternately, the electron beam could be turned off and oxygen admitted to the system, producing UO_2^+ via Reaction (2). The uranium dioxide signal was similarly measured, and is related to the cross section by

$$S_a = \sigma_a n_{O_2} l_a e \bar{v}_U n_U A_U , \quad (8)$$

where the subscript "a" refers to the associative ionization process, n_{O_2} is the oxygen number density as measured by a nude ionization gauge, calibrated for oxygen against a McLeod gauge, suitably dry ice trapped to eliminate the Ishii-Nakayama effect of mercury pumping, l_a is the associative ionization path length, e is the electronic charge, $\bar{v}_U$ is the mean velocity of the uranium beam averaged over the number density, and A_U is the effective cross-sectional area of the uranium beam at the interaction region. The last three terms together can be thought of as defining a "uranium atom current." A similar expression,

$$S_i^U = \sigma_e^U I_e n_U l_i^U , \quad (9)$$

can be written for the electron-impact ionization of uranium. Equations (8) and (9) are combined to give

$$\frac{\sigma_e^U}{\sigma_a} = \frac{S_i^U}{S_a}\frac{n_{O_2}}{I_e}\frac{\bar{v}_U e A_U l_a}{l_i^U}. \quad (10)$$

The details are given in the Appendix. If one knows the value of σ_a, the absolute cross sections σ_e^U are determined from Eq. (10).

In the present experiments the value for σ_a was taken as $(4.01 \pm 0.55) \times 10^{-17}$ cm^2, which is the most recently determined value of the effective cross section for Reaction (2) as measured in an experiment[10] in which a Maxwellian beam of U atoms passes through a Maxwellian gas of O_2, at the temperatures used in the present experiment. This value is higher than a value reported previously.[8]

III. EXPERIMENTAL APPARATUS

A. Basic apparatus

The basic experimental apparatus shown in Fig. 1 is similar to that used previously in this laboratory[17-19] except that no getter pump was used to improve the vacuum, only a simple liquid nitrogen cyropump.

The urnaium beam was produced in the first of three differentially pumped vacuum chambers by joule-heating a tubular furnace made by rolling a strip of tungsten foil, in which a small (~0.5 g) piece of uranium metal was placed. A 2-mm hole sandblasted in the wall permitted molten uranium to creep out and coat much of the surface from which the uranium evaporated to form a fairly wide beam. The hole also permitted reloading of the furnace; however, at most two but usually only one run was possible before the furnace succumbed to attack from the liquid uranium.

The beam entered the second chamber where it was chopped by a toothed wheel at a frequency of 19 Hz. This unusually low frequency was necessary because of the large (10^9 Ω) input resistence of the preamplifier. In order to prevent large signal attenuation, the modulation period must be of the order of or larger than the time constant of the amplification circuitry. The intrinsic capacitance of the preamplifier was ~25 pF, giving a time constant of $\sim 2.5 \times 10^{-2}$ sec. At 19 Hz, the signal attentuation was approximately $3dB$.

The atom beam passed through a 3-mm diameter aperture into the third chamber, where it was further collimated and shaped, and then intersected by a well-defined electron beam. The ions produced were collected, recorded, and analyzed, as described in the next two subsections.

1. Ionizer and quadrupole

For the measurements of the relative cross sections for the individual ion charge states, the apparatus shown in Fig. 2 was used. The electron source was a crossed-beam ionizer that produced a focused beam of electrons 2-mm diameter at the interaction region with currents of 0.5-5 μA and an energy spread of 0.5 eV. The remainder

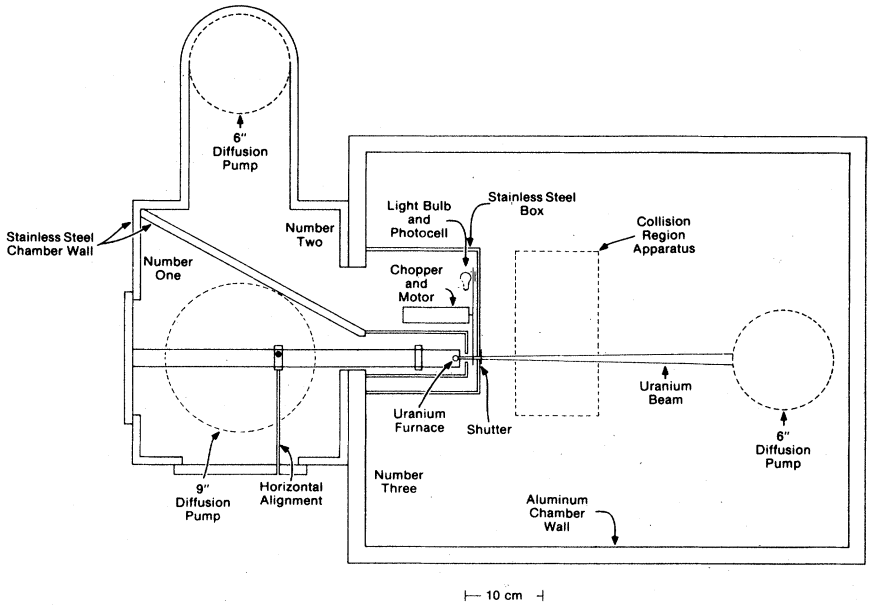

FIG. 1. Vacuum system, showing uranium beam source and approximate position of the collision region apparatus.

of the ionizer extracted the ions from the interaction region, focused them, and directed them into a QMF (Extranuclear Model 324-9) which selected the particular ion to be studied. The QMF was placed perpendicular to the uranium beam to eliminate spurious signals caused by neutral uranium undergoing associative ionization with background oxygen in the vicinity of the electron multiplier. A venetian blind type electron multiplier (SRC Model EM-2101) at the exit end of the QMF amplified the signal from the selected ions.

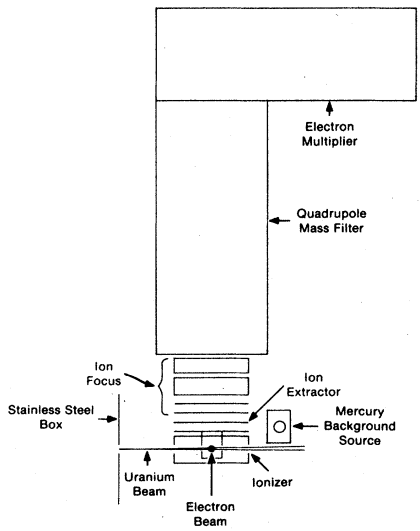

FIG. 2. Ionizer and quadrupole mass filter for the cross-section ratio and shape measurements.

2. Electron gun and parallel plates

For the measurement of the total cross section, a simple electron gun similar to others used in this laboratory[17] was used. The electrons were produced by heating a tungsten ribbon $0.5 \times 0.025 \times 6$ mm^3. The filament was negatively biased so that the electron energy was determined by the potential difference between the anode at ground potential and the filament. In order to assure that the entire electron beam would pass through the uranium beam, it was necessary to use a magnetic field of 60 G to help focus the electrons. A two-stage Faraday collector was used to measure the electron current. The collector consisted of a plate 5 cm from the gun's anode with a 3-mm hole to allow passage of electrons, and a cylinder 2.2 cm in diameter, closed at one end, located directly behind the hole in the plate. The electron beam was focused so that the current to the plate was <0.1% of that to the tube; thus the beam had a diameter < 3 mm at the interaction region. From these parameters, it is calculated that the increase in electron path length due to their helical motion in the magnetic collimating field was no more than 3% for electrons with energy in excess of 100 eV.[20] Typically, the electron current at this energy was about 100 μA.

The collision region, shown in Fig. 3, consisted of a set of parallel plates, 2×10 cm$^2 \times 1.6$ mm, with a 75% transmission gold mesh placed between them. The bottom plate and the mesh, 2-cm apart,

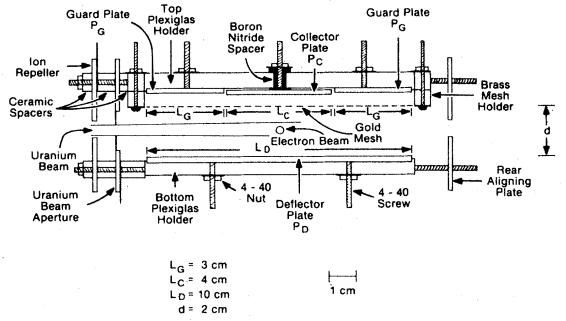

FIG. 3. Parallel-plate collision region for the absolute cross-section measurements.

were biased so that the center of the region was at ground potential and the ions would be accelerated upward through the mesh. This grounding arrangement was used so that the potentials on the Faraday collectors and collimators would not have to be adjusted as the electron energy was changed. As the potential difference between the bottom plate and the mesh was increased, the ion signal reached a plateau; an electric field of 8 V/cm was sufficient to assure complete saturation.

The upper plate actually consisted of three parts: a center collection plate connected to an electrometer, the feedback of which kept the potential on the plate to within one milivolt of the potential at which the electrometer was biased, and two outer guard plates (each 3-cm long) biased at the same potential as the electrometer. The electrometer and thus the plates were negatively biased in order to prevent scattered electrons from reaching the collector. With the plates at the same potential as the filament, no electrons were collected. The signal remained constant as the potential was increased as much as 200-300 V, an evidence that no secondary electrons were lost in the measurement. The guard plates were used to provide a uniform field at the edges of the collector in order to define accurately the uranium path length for associative ionization measurements.

The three apertures in Fig. 3 (from left to right) served to repel positive ions from the furnace, collimate the uranium beam to the desired shape and size, and aid in alignment of the apparatus. To assure the validity of the data, several measurements of the ion currents were made with varying electron currents and oxygen pressures. The ion signals were linear with respect to both of these parameters. As there was no direct means of measuring the uranium beam density, only qualitative observations of its effect on the ion signals were possible.

IV. RESULTS AND DISCUSSION

The cross-section ratios in Eqs. (4) and (5) were measured several times at various energies. The value for each point was taken to be the mean of between six and fifteen measurements of that ratio, with an uncertainty of one standard deviation of those measurements. From these ratios, the absolute cross sections σ^U_{n+} were determined; they are shown in Fig. 4 and in Table II. The uncertainties in the ratios were combined in quadrature to yield the listed uncertainties. In most cases, the chief contribution to the uncertainty was from the ratio of Eq. (5), the shape of the σ^U_+ curve. Also, there is an overall uncertainty of 17% in the scale of all the cross sections in Table II, due to a 14% uncertainty in σ_a and a 10% uncertainty in the total cross-section measurement relative to σ_a. This scale uncertainty also holds for Fig. 5 and for the present data in Fig. 6.

The curves of σ^U_{n+} all exhibit a shape typical of process: a rapid rise from threshold, a maximum occurring at about three to five times the appearance potential, and a slow fall thereafter. (See for example Kieffer[16] or Tate and Smith.[21]) As n increases, the rise becomes less rapid and the peak broadens from a fairly narrow one at $n=1$ to a very wide one at $n=4$.

The cross sections σ^U_e and σ^U_{ion} are also given in Table II and displayed in Fig. 5. In Fig. 6, the present result σ^U_{ion} is compared to calculations that are based on formulas given by Mann,[13] Gryzinski,[14] and Lotz.[15] Mann's method is a semi-empirical approach using the mean square radii of the various shells and an $(\ln x)/x$-type energy dependence, where $x=E/V_i$, E is the electron energy and V_i is the ionization potential

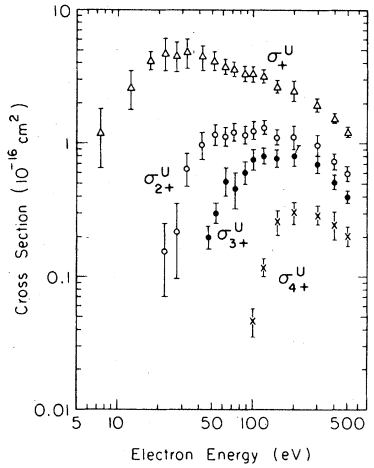

FIG. 4. Cross sections for electron-impact ionization of U leading to U^+, U^{2+}, U^{3+}, and U^{4+}.

TABLE II. Experimental electron-impact ionization cross sections of uranium. All cross sections are in units of 10^{-16} cm^2 and have an overall uncertainty of 17%. The numbers in parentheses give the statistical uncertainties in the last few places of the preceding number.

E(eV)	σ_+^U	σ_{2+}^U	σ_{3+}^U	σ_{4+}^U	σ_e^U	σ_{ion}^U
7.5	1.23(58)				1.23(58)	1.23(58)
12.5	2.66(88)				2.66(88)	2.66(88)
17.5	4.23(64)				4.23(64)	4.23(64)
22.5	4.80(127)	0.16(9)			5.12(134)	4.99(128)
27.5	4.55(117)	0.22(13)			5.04(127)	4.82(118)
32.5	4.78(114)	0.64(18)			6.07(144)	5.45(127)
37.5	4.69(110)	0.88(29)			6.45(148)	5.60(122)
42.5	4.42(90)	0.98(23)			6.39(128)	5.39(106)
47.5	4.75(73)	1.20(23)	0.20(4)		7.74(117)	6.13(90)
52.5	4.26(67)	1.14(19)	0.30(5)		7.45(117)	5.71(90)
57.5	3.94(44)	1.10(15)	0.37(5)		7.27(81)	5.45(58)
62.5	3.76(47)	1.13(15)	0.52(12)		7.59(88)	5.39(58)
67.5	3.71(55)	1.19(19)	0.45(16)		7.45(102)	5.39(63)
72.5	3.62(42)	1.22(16)	0.46(13)		7.88(80)	5.66(47)
77.5	3.47(36)	1.23(19)	0.51(8)		7.74(73)	5.39(47)
82.5	3.46(39)	1.23(13)	0.51(11)		7.81(80)	5.08(46)
87.5	3.26(32)	1.17(15)	0.62(12)		8.03(73)	5.45(42)
92.5	3.19(51)	1.18(20)	0.63(18)		7.88(117)	5.28(71)
100	3.23(15)	1.23(15)	0.77(13)	0.05(1)	8.18(36)	5.29(18)
110	3.12(21)	1.23(17)	0.83(7)	0.09(1)	8.47(51)	5.29(26)
120	3.11(24)	1.33(14)	0.82(12)	0.12(2)	8.69(58)	5.39(31)
130	3.04(30)	1.25(13)	0.80(15)	0.17(5)	8.61(73)	5.26(34)
140	2.93(34)	1.31(26)	0.78(14)	0.18(3)	8.61(88)	5.18(47)
150	2.66(28)	1.10(17)	0.78(12)	0.26(5)	8.25(80)	4.83(44)
175	2.56(40)	1.11(21)	0.79(13)	0.26(6)	8.18(124)	4.74(68)
200	2.50(44)	1.12(23)	0.81(15)	0.31(6)	8.40(146)	4.77(81)
250	2.03(21)	1.06(16)	0.67(11)	0.28(4)	7.27(69)	4.04(34)
300	1.96(25)	0.98(18)	0.69(9)	0.30(5)	7.18(86)	3.93(44)
400	1.55(13)	0.75(10)	0.52(6)	0.25(6)	5.61(40)	3.07(14)
500	1.21(11)	0.60(9)	0.41(4)	0.21(4)	4.45(37)	2.42(17)

of the ith shell. The contributions to the cross section for the $5f$, $6d$, and $7s$ shells of uranium were calculated and added together for the net results. Lotz's method utilizes a similar energy dependence but uses a weighted average for V_i based on the ionization potentials and number of

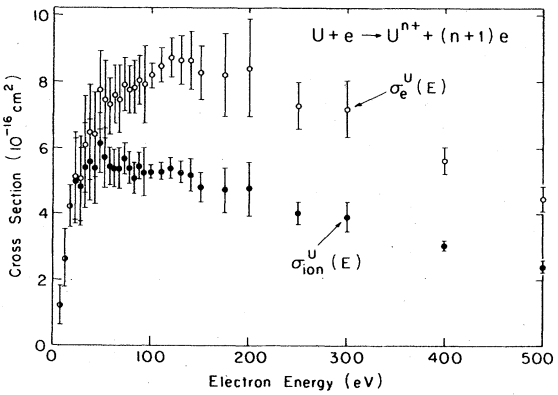

FIG. 5. Total ionization cross sections: ○, $\sigma_e^U(E) = \Sigma n \sigma_{n+}^U(E)$; ●, $\sigma_{ion}^U(E) = \Sigma \sigma_{n+}^U(E)$.

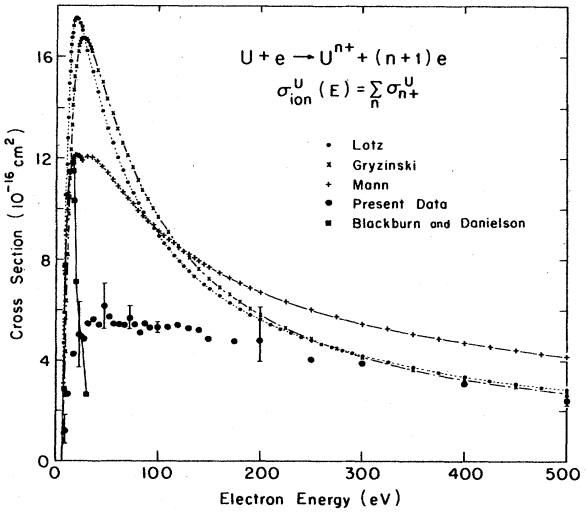

FIG. 6. Comparison of theoretical calculations and experimental results for the total ionization cross section σ_{ion}^U. Theoretical: +, Mann (Ref. 13); ×, Gryzinski (Ref. 14); ●, Lotz (Ref. 15). Experimental: ●, present data; ■, Blackburn and Danielson (Ref. 12). The latter's results are normalized at 15 eV to Mann's.

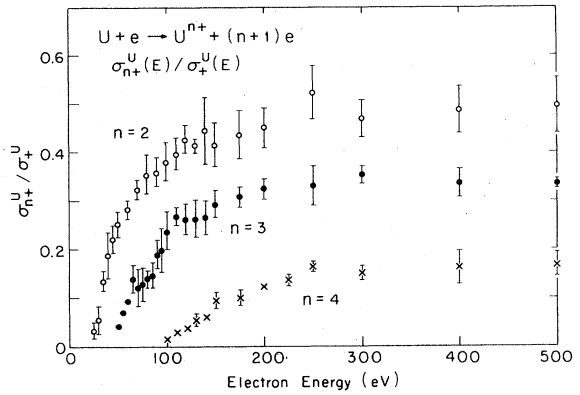

FIG. 7. Ratios of the cross sections for multiple ionization, σ^U_{n+}, to single ionization, σ^U_+: ○, $n=2$; ●, $n=3$; ×, $n=4$.

electrons in each shell. Gryzinski derived a formula based on classical two-body collision theory. From these formulas, the authors calculated the contribution for each of the three outer shells and added them together for the net results.

These three calculations ostensibly are for σ^U_+, but this is not the case. None of the calculations makes any correction for possible multiple ionizations. This correction would reduce the calculated value by the amount that is lost to higher ionizations. Instead, any ions that have been multiply ionized must be included with singly ionized ones. Consequently, the calculations are actually for σ^U_{ion}.

The agreement of the present data with all

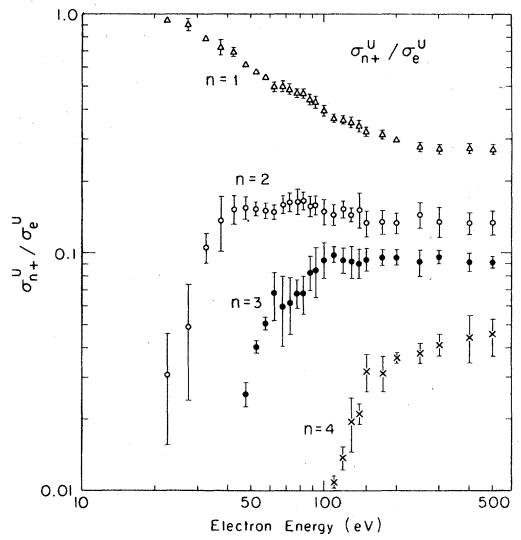

FIG. 8. Ratios of the multiple ionization cross sections to the total cross section, σ^U_{n+}/σ^U_e: △, $n=1$; ○, $n=2$; ●, $n=3$; ×, $n=4$.

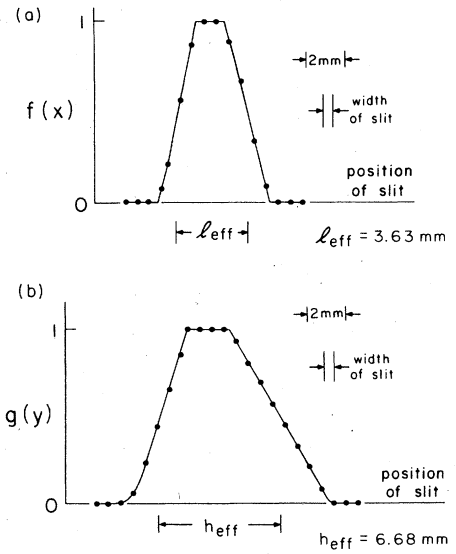

FIG. 9. Beam profile measurements for the uranium atom beam. Slit width = 0.508 mm. (a) Along axis of electron beam (i.e., width), $l_{\text{eff}} = 3.63$ mm. (b) Perpendicular to electron beam (i.e., height), $h_{\text{eff}} = 6.68$ mm.

three calculations is reasonable at energies above 250 eV. At lower energies, the Lotz and Gryzinski formulas overestimate the contributions from the d and f shells, hence the higher values. Lin and Stafford[22] have found that in general, Mann's formula gives lower values than Gryzinski's formula and tends to have much better agreement with experimental data. The present data exhibits a maximum about 50% lower in magnitude at an energy about 15 eV higher than that from Mann. This degree of difference is not necessarily alarming as the estimates of the mean square radii of the orbitals given by Mann may be in error, and the type of contribution of each shell is based on fitting calculations to experimental data and may not be valid for uranium. Consequently, the calculations, especially at low energies, are not reliable without further study.

Also displayed in Fig. 6 is the cross section for single ionization of uranium atoms measured by Blackburn and Danielson,[12] normalized at 15 eV to Mann. In their experiment, uranium and uranium oxide beams were produced from a tungsten Knudsen cell. The beams passed through the ionizer of a quadrupole mass spectrometer, and the ions and fragments were then analyzed. Corrections were made in the U^+ case for ions formed by fragmentation of UO; however, measurements were too imprecise to permit correction for U^+ from UO_2 (only occurring at energies greater than 22 eV). For the energy range of this data, the correction for multiple ionization is negligible.

This data shows a maximum at 15 eV, significantly lower than the calculated or measured energies for the maximum (20-27 eV). There is also a very rapid drop off in cross section at energies above the maximum. This drop is much sharper than for the present data and calculations given here. No example could be found in the literature of a cross section for single ionization of an atomic species by electron impact that exhibited such a rapid drop.

Figure 7 displays the ratios $\sigma_{n+}^{U}/\sigma_{+}^{U}$, the relative amounts of multiply ionized uranium compared to singly ionized. Figure 8 gives the ratios $\sigma_{n+}^{U}/\sigma_{e}^{U}$, the relative amount each ion charge state contributes to the total cross section. These ratios, particularly for $n=3$ and 4, have a maximum several times larger than for all other species that have been studied, except as noted below.

The only elements with cross-section ratios that are comparable to the present results for which electron-impact ionization data are available are the alkaline earths, which have a second ionization cross-section ratio about the same as the uranium. For $n=3$ or 4, uranium has a cross-section ratio about an order of magnitude or more larger than any element except barium; the ratio for barium is about half that of uranium for $n=3$ and a third for $n=4$.

The alkaline earths are similar in that there are two s electrons loosely bound in the outer shell. The main difference is that uranium has a third electron, $6d$, with about the same binding energy as the $7s$ electrons. The elements closest in structure to which comparisons can be made are the III B elements: Sc, Y, La, Ac, and the rare earths. Unfortunately, no experimental results are available for these elements.

ACKNOWLEDGMENT

This work was supported in part by the U.S. Department of Energy under Contract No. EN-77-S-02-4295.A000.

APPENDIX

When determining path lengths in a crossed-beam experiment, one must be careful to account for variations in beam density in the reaction volume. For example, of one-dimensional beam A crosses a nonuniform three-dimensional beam B, the reaction cross section σ is related to the product signal S_p by

$$S_p=\sigma I_A \int n_B(x)dx\,, \tag{A1}$$

where I_A is the current of beam A, $n_B(x)$ the number density of beam B in the x direction, and S_p and I_A are in like units, e.g., particles/sec. From this equation one can define an effective path length, l_{eff}, by

$$l_{\text{eff}}\, n_0 = \int n(x)dx\,, \tag{A2}$$

where n_0 is some appropriately chosen number density. For a simple three-dimensional beam in which the central portion is uniform (the usual case), n_0 would be the density at the center. The distribution $n(x)$ can be determined by beam profile measurements. This can be generalized for three-dimensional beams and for beams through gas.

In the present study, Eq. (9), when correctly written, is

$$S_i=\sigma_e \iiint_{\text{interaction volume}} n_U(x,y,z)j(x,y,z)dx\,dy\,dz\,, \tag{A3}$$

where the electron beam cross section is in the yz plane, the uranium beam cross section is the xy plane, and j is the electron beam current density.

For simple geometries, such as a rectangular beam from a small uniform density source as in the present case, the number density of the uranium beam can be separated into functions of x, y, and z:

$$n_U(x,y,z)=n_0 f(x)g(y)h(z)\,. \tag{A4}$$

For the dimensions used in this study, the $1/r^2$ character of the density in the z direction is negligible, hence $h(z)\equiv 1$ in the interaction region. The beam profile was measured by placing a narrow travelling slit at the interaction region of the parallel plate arrangement, introducing oxygen into the system, and monitoring, as in Sec. III A, the UO_2^+ signal beyond the slit as the slit was swept across the beam cross section. Measurements were made in the x and y directions; the results are illustrated in Fig. 9.

The central part of the uranium beam is uniform in the xy plane and monotonically decreases to zero at the edges. The entire electron beam crossed the central region with respect to the y direction [i.e., where $g(y)\equiv 1$]. Thus one obtains

$$\begin{aligned} S_i &= \sigma_e \int n_U(x)\left(\iint_{\text{electron beam}} j(x,y,z)dy\,dz\right)dx \\ &= \sigma_e I_e \int n_U(x)dx\,. \end{aligned} \tag{A5}$$

Similarly, Eq. (8) becomes

$$S_a=\sigma_a n_{0_2} \iiint_{\text{interaction volume}} J\,dx\,dy\,dz\,, \tag{A6}$$

where J is the uranium beam current density. Because the interaction region is sufficiently short compared to the distance from the furnace, $1/r^2$ effects are negligible, the "z" integral merely gives the interaction path length l_a. Using the definition of "uranium atom current" given with Eq. (8),

$$S_a = \sigma_a n_{0_2} l_a \bar{v}_U e \iint n_U(x,y)\,dx\,dy\,, \tag{A7}$$

where the integral defines an effective area similar to the definition of effective path length in Eq. (A2). Combining Eqs. (A4), (A5), and (A7), one obtains

$$\frac{\sigma_e}{\sigma_a} = \frac{S_i}{S_a}\frac{n_{0_2} l_a \bar{v}_U e}{I_e}\frac{n_0 \int f(x)dx \int g(y)dy}{n_0 \int f(x)dx}$$

$$= \frac{S_i}{S_a}\frac{n_{0_2} l_a \bar{v}_U e}{I_e}\int g(y)dy\,, \tag{A8}$$

where $\int g(y)\,dy$ defines an effective height of the uranium beam. This height was measured as described above. The height can also be calculated in simple geometries. Note the unusual result that the cross-section ratio is independent of the path length of the electron beam through the uranium beam.

---

*Present address: Sachs/Freeman Associates, Inc., Bowie, Md. 20715.
†Present address: Extranuclear Laboratories, Inc., P.O. Box 11512, Pittsburgh, Pa. 15238.

[1]D. W. Steinhaus, L. J. Radziemski, Jr., R. D. Cowan, J. Blaise, G. Guelachvili, Z. B. Osman, and J. Verge, LASL Report No. LA-4501, 1971 (unpublished).
[2]J. Blaise and L. J. Radziemski, Jr., J. Opt. Soc. Am. 66, 644 (1976).
[3]J. B. Mann, J. Chem. Phys. 40, 1632 (1964).
[4]I. N. Bakulina and N. I. Ionov, Zh. Eksp. Teor. Fiz. 36, 1001 (1959). [Sov. Phys.–JETP 9, 709 (1959)].
[5]J. Sugar, J. Chem. Phys. 59, 788 (1975).
[6]S. Sinha and J. N. Bardsley, Phys. Rev. A 14, 104 (1976).
[7]H. H. Lo and W. L. Fite, unpublished experimental results.
[8]W. L. Fite, H. H. Lo, and P. Irving, J. Chem. Phys. 60, 1236 (1974).
[9]C. E. Young, P. M. Dehmer, R. B. Cohen, L. G. Pobo, and S. Wexler, J. Chem. Phys. 65, 2562 (1976).
[10]J. C. Halle, H. H. Lo, and W. L. Fite, J. Chem. Phys. 73, 5681 (1980).
[11]W. L. Fite, T. A. Patterson, and M. W. Siegel, AFGL Report No. AFGL-TR-77-0030, Air Force Geophysics Laboratory, Air Force Systems Command, USAF, Hanscom AFB, Mass., 01731, 1976 (unpublished).
[12]P. E. Blackburn and P. M. Danielson, J. Chem. Phys. 56, 6156 (1972).
[13]J. B. Mann, J. Chem. Phys. 64, 1646 (1967).
[14]M. Gryzinski, Phys. Rev. 138A, A366 (1965).
[15]W. Lotz, Astrophys. J. Suppl. 14, 207 (1967).
[16]L. J. Kieffer, At. Data 1, 19 (1969).
[17]W. R. Ott, W. E. Kauppila, and W. L. Fite, Phys. Rev. A 1, 1099 (1970).
[18]T. Kondow, R. J. Girnius, Y. P. Chong, and W. L. Fite, Phys. Rev. A 10, 1167 (1974).
[19]Y. P. Chong and W. L. Fite, Phys. Rev. A 16, 933 (1977).
[20]H. S. W. Massey and E. H. B. Burhop, *Electronic and Ionic Impact Phenomena*, 2nd ed. (Oxford University Press, London, 1969), Vol. 1, p. 101.
[21]J. T. Tate and P. T. Smith, Phys. Rev. 46, 773 (1934).
[22]S. S. Lin and F. E. Stafford, J. Chem. Phys. 48, 3885 (1968).